mining

MDPI

Article

An Autochthonous *Acidithiobacillus ferrooxidans* Metapopulation Exploited for Two-Step Pyrite Biooxidation Improves Au/Ag Particle Release from Mining Waste

Andrea E. Jiménez-Paredes *, Elvia F. Alfaro-Saldaña *, Araceli Hernández-Sánchez and J. Viridiana García-Meza

Geomicrobiología, Facultad de Ingeniería-Metalurgia, UASLP Unidad de Posgrado e Investigación, Sierra Leona 550, Lomas 2°, San Luis Potosí 78210, Mexico; aracelihersan@gmail.com (A.H.-S.); jviridianagm@gmail.com (J.V.G.-M.)

* Correspondence: jimenez.andreaelena@gmail.com (A.E.J.-P.); elvia.saldana@uaslp.mx (E.F.A.-S.)

Abstract: Pyrite bio-oxidation by chemolithotrophic acidophile bacteria has been applied in the mining industry to bioleach metals or to remove pyritic sulfur from coal. In this process, it is desirable to use autochthonous and already adapted bacteria isolated directly from the mining sites where biomining will be applied. Bacteria present in the remnant solution from a mining company were identified through cloning techniques. For that purpose, we extracted total RNA and performed reverse transcription using a novel pair of primers designed from a small region of the 16S gene (V1–V3) that contains the greatest intraspecies diversity. After cloning, a high proportion of individuals of the strains ATCC-23270 (NR_074193.1 and NR_041888.1) and DQ321746.1 of the well-known species *Acidithiobacillus ferrooxidans* were found, as well as two new wild strains of *A. ferrooxidans*. This result showed that the acidic remnant solution comprises a metapopulation. We assayed these strains to produce bioferric flocculant to enhance the subsequent pyrite bio-oxidation, applying two-stage chemical–bacterial oxidation. It was shown that the strains were already adapted to a high concentration of endogenous Fe^{2+} (up to 20 $g \cdot L^{-1}$), increasing the volumetric productivity of the bioferric flocculant. Thus, no preadaptation of the community was required. We detected Au and Ag particles originally occluded in the old pyritic flotation tailings assayed, but the extraction of Au and Ag by cyanidation resulted in ca. 30.5% Au and 57.9% Ag.

Keywords: cloning; metapopulation; *A. ferrooxidans* strains; preoxidation; bioferric; biomining

Citation: Jiménez-Paredes, A.E.; Alfaro-Saldaña, E.F.; Hernández-Sánchez, A.; García-Meza, J.V. An Autochthonous *Acidithiobacillus ferrooxidans* Metapopulation Exploited for Two-Step Pyrite Biooxidation Improves Au/Ag Particle Release from Mining Waste. *Mining* **2021**, *1*, 335–350. https://doi.org/10.3390/mining1030021

Academic Editors: Sebastien Farnaud and Eva Pakostova

Received: 5 October 2021
Accepted: 17 November 2021
Published: 29 November 2021

1. Introduction

At this point in time, metal recovery mining is facing its greatest challenge: to find new extractive methods for occluded or refractory metals, due to the current difficulty of locating high-grade ores. In addition to this issue, there are new concerns about environmental protection and conservation, and the need to reduce costs and energy consumption in mining companies. These concerns are best solved by using biomining methods or "biohydrometallurgy" [1,2], as the advantages are (1) no emissions into the atmosphere, (2) the low cost of operation and installation, (3) regeneration of the reagent used (Fe^{3+}) by microorganisms and recirculation of the solution (to reuse water, acidity and Fe^{3+}), and (4) the process takes place at ambient temperature and pressure.

Biohydrometallurgy is based on microbially catalyzed processes or bio-oxidation to extract metals by dissolving ores into acidic aqueous solutions (bioleaching) [3–5]. The bio-oxidation may accelerate the oxidation of the Fe^{2+} released during pyrite (FeS_2) oxidation by a factor of 10^6 [6]. The microorganisms used in biohydrometallurgy procedures must be able to grow autotrophically at low pH, assimilate inorganic carbon, and resist soluble metals [7].

FeS_2 is the most abundant metal sulfide in the Earth's crust [8]. FeS_2 arouses the economic interest of the extractive mining sector when it is associated with ores containing

Au and Ag. However, Au and Ag may be in a "refractory" state, a condition that prevents cyanide solutions from contacting them, considerably limiting their recovery using conventional cyanidation techniques [9]. Trace elements and precious metals can be liberated by bio-oxidation [4,10]. Some studies have suggested preoxidation of the mineral prior to its bio-oxidation [11,12] as a simple, cheap, and harmless method to achieve higher efficiency in subsequent bio-oxidation for refractory sulfidic concentrates containing noble metals such as Au [13].

The two-stage chemical–bacterial oxidation of metal sulfides has been used as an alternative pretreatment for efficient recovery of Au, since chemical preoxidation may provide short-term preprocessing of the energetic substratum for its subsequent bio-oxidation in the second stage of the process [13–18]. Because temperature influences the catalyzation of the sulfide oxidation [19], sulfidic elements are removed from the mineral concentrate Equation (1) if the initial chemical stage occurs at >70 °C. The second stage of bio-oxidation over the solid remnant enables Fe^{3+} regeneration Equation (2) and bio-oxidation of reduced sulfur compounds such as S^0 Equation (3), increasing Au recovery from the FeS_2 concentrate.

$$SM + 2Fe^{3+} \rightarrow M^{2+} + S^0 + 2Fe^{2+} \quad (1)$$

$$4Fe^{2+} + 4H^+ + O_2 \rightarrow 4Fe^{3+} + 2H_2O \quad (2)$$

$$2S^0 + 3O_2 + 2H_2O \rightarrow 2H^+ + 2SO_4{}^{2-} \quad (3)$$

Bacteria such as *A. ferrooxidans* oxidize the Fe^{2+} Equation (2) and directly oxidize the reduced sulfur compounds Equation (3), due to their sulfur oxidation capacity [20].

Bio-oxidation has been proposed as an attractive technique due to its low environmental impact. Specifically, it has been proposed to use bacteria present in the mine's processing solutions (e.g., remnant solutions), since bio-oxidation is more efficient if an endemic bacterium is used instead of an allochthonous single-strain population [5,21]. Bacteria for biohydrometallurgy can be used either as a community composed of different species or as a metapopulation of one single known species. The term "metapopulation" refers to "a set of local populations inhabiting discrete habitat patches that are connected to one another through dispersal or migration" [22]. Even though the concept of a "metapopulation" was first conceived for animals and plants, it has also been used in analyses of bacterial dynamics [23], including acid mine drainage research [24]. Bacterial populations undergo recombination processes that generate individuals whose genomes have different population histories and populations with recombination-derived mosaicism [25]. These genetic processes assist individuals and the overall population to adapt and thrive in their habitat. Thus, genomic changes that follow stochastic events of mutation, recombination, insertion, or deletion [26,27] ultimately compose a whole metapopulation. In biohydrometallurgical batches, the dominant strains are usually the indigenous strains because the deep oxidative processes in these pulps activate microevolutionary processes and give rise to new strains that differ in terms of "the structure of chromosomal DNA, plasmid composition, optimal pH and temperature for growth, the growth and substrate oxidation rates, resistance to heavy metal ions, adaptability and adaptation thresholds" [28].

In this work, the main bacteria species from an industrial remnant solution was identified by 16S mRNA and used for microbial oxidation of FeS_2-rich material from ZnS flotation; currently, these tailings are stored as mining wastes that are suitable for being exploited due to their content of Au. To ensure FeS_2 oxidation, a two-stage chemical-bacterial oxidation was assayed in this work.

2. Materials and Methods

2.1. Pyrite Concentrate

Mining waste deposits (old pyritic flotation tailings) were used. This waste was mainly composed of FeS_2 (52.2%) and other sulfurs (20.7%), including sphalerite (ZnS) and galena (PbS). The FeS_2 contained occluded Ag and Au particles, up to 78 g Ag/T and 22.4 g Au/T (Table 1). The 92% class fineness was <53 μm.

Table 1. Metal content in FeS_2 concentrate.

Element	Fe	Cu	Zn	As	Pb	Ag	Au
			(%)			(g/T)	
Content	36.2	0.04	0.30	0.46	0.23	78	22.4

To measure the total concentration of metals, the FeS_2 concentrate was digested in acid media (a 3:1 ratio of concentrated HNO_3 and HCl), and the extracted solution was filtered through a cellulose acetate syringe filter with a 0.45 µm pore size (Advantec 03CP045AN). The concentrations of Fe, Cu, Zn, Pb, As, and Ag were analyzed by an atomic absorption spectrophotometer with a graphite furnace (Perkin Elmer). For Au, the solution was analyzed by inductively coupled plasma optical emission spectrophotometry (ICP-OES). Other metals in the concentrates are presented in Table 1.

2.2. Origin, Acquisition, and Maintenance of Microorganisms

The bacteria were obtained from a remnant solution (T6) from biohydrometallurgical processing that was delivered by a mining company. The solution was used to generate ferric ions (Fe^{3+}) by ferrous bio-oxidation (Fe^{2+}). T6 was analyzed for the density of active (mobile) cells, pH, ORP, and total Fe and Fe^{2+} concentrations. This community was not incubated; instead, it was used directly from the solution delivered by the company, which was considered to have been discarded from their process.

To isolate the original bacterial community from the T6 solution (named T6-OC), a separation method was standardized. Non-incubated samples from the bottom of the container were obtained, where precipitate particles had formed, so cells were separated from the residues by centrifugation (twice at 21,000× *g* and 4 °C per 1.5 min) and pellets were washed in acidified water (with concentrated H_2SO_4 at pH 1.5) to dissolve the precipitates. The cell samples obtained were used for identification and culture.

The bacteria were cultured in triplicate in modified K9 (Km) medium [29] containing, per liter of deionized water, 0.4 g of $MgSO_4 \cdot 7H_2O$, $(NH_4)_2SO_4$, and KH_2PO_4; 14 g Fe^{2+} (as $FeSO_4 \cdot 7H_2O$, added through a sterilizing filter using a 0.22 µm pore-size polycarbonate filter); and 2.0 g of S^0. The initial pH was fixed at 1.8 (with H_2SO_4, 98%). The cultures were maintained at 160 rpm and 30 ± 1 °C until use (3–4 weeks).

To adapt the cultured bacteria to the 10% FeS_2 concentrate (*w*/*v*), the microorganisms were exposed to a progressive increase in the concentrate content (2%, 6%, 8%, and 10%). Previously, the FeS_2 concentrate was finely ground to ≤37 µm (sieve mesh 400) as the recommended particle size for bio-oxidation is 25 to 45 µm [30]. Each assayed stage was performed in triplicate in Erlenmeyer flasks with Km medium (pH 1.8) and an initial cell density of 10^7 cells·mL^{-1}. The cultures were incubated for 14 days at 30 ± 1 °C with constant agitation (120 rpm). Bacteria for the bio-oxidation assays were obtained from the final culture (with 10% FeS_2 concentrate) and were named the T6-adapted culture (T6-AC).

2.3. Identification of Bacteria

Subsamples of cells isolated directly from T6 (T6-OC) and subsamples of cells from the adapted culture (T6-AC) were centrifuged again and washed with a saline phosphate buffer (PBS) (8.06 g NaCl, 0.22 g KCl, 1.15 g Na_2HPO_4, and 0.2 g KH_2PO_4 dissolved in 1 L deionized water and filtered for sterilization). From this, solutions with ~2.5 × 10^9 cells·mL^{-1} were achieved, and the cells were concentrated using PBS (21,000× *g* and 4 °C per 1.5 min).

In the present work, we identified the bacteria using RNA extraction and reverse transcription of the V1–V3 region of the 16S gene, and further cloning. For this purpose, primer pair was selected. A bioinformatic study was carried out using the 16S universal bacterial primers proposed by Callender et al. [31] and Mesa et al. [32]. These were selected due to their similarity in environmental conditions, being gold mine waste rocks and tailings, and drainage from an acid mine, respectively. In both studies, the authors identified a bacterial community amplifying the region between V1 and V3 of the 16S gene. Marchesi et al. [33] designed a pair of universal 16S bacterial primers targeted for use with complex natural

samples, so these were also selected as possible primers to use in the present study. The universal 16S primers from these three studies [31–33] were analyzed using the BLAST bioinformatics tool [34] (Available online: https://blast.ncbi.nlm.nih.gov; 1 February 2019) versus the 16S sequences reported in GenBank for species of acidophilic bacteria. Following this, the pair of primers with the highest number of alignments was selected. The chosen primers were the forward primer F63 (CAGGCCTAACACATGCAAGTC) from Marchesi et al. [33] and the reverse primer R533 (ATTACCGCGGCTGCTGGC) from Callender et al. [31]. The bioinformatic study of these two primers together resulted in the amplification of 22 species in total of the genera *Acidimicrobium*, *Acidiphilium*, *Acidithiobacillus*, *Acidobacterium*, *Desulfurella*, and *Leptospirillum* (Table S1). Thus, this pair of primers gave the highest number of matches with 22 acidophilic species. All expected amplicons from these 22 species (Table S1) ranged between 404 and 516 bp and amplified a fragment between the V1 and V3 regions of the 16S gene. These have been shown to effectively identify bacteria [35,36] as V1 and V2 contain the greatest intraspecies diversity [37], and the region V1–V3 has been used in other work to identify acidophile microorganisms [31,32,38,39]. The primers were synthesized by T4 Oligo (synthetic cycle method, Mexico), resuspended at 50 $\mu g \cdot \mu L^{-1}$, and stored at −20 °C until use.

rRNA extraction and reverse transcription into 16S rDNA (named complementary DNA) were performed by reverse transcription–polymerase chain reaction (RT-PCR) using the chosen primers. RT-PCR was chosen to identify acidophile bacteria because of its specificity and sensitivity that ensures the optimal DNA reverse amplification; also, rRNA extraction provides more copies of the 16S coding region. Cells concentrated in PBS were used to extract RNA using TRIzol reagent (Invitrogen, Waltham, MA, USA) following the manufacturer's protocol; reverse transcription was performed with 0.5 µg of extracted RNA in a reaction with a total volume of 20 µL according to the instructions of the manufacturer of the 200U M-MLV (Invitrogen, USA). A GoTaq Flexi DNA Polymerase (Promega, Madison, WI, USA) kit was used for PCR reactions following the instructions recommended by the supplier, using the primers F63 and R533 and an annealing temperature of 72 °C (Labnet MultiGene OptiMax). PCR products were analyzed by electrophoresis in 1% agarose gels (Sigma-Aldrich, St. Louis, MO, USA). Bands obtained with the expected size of 16S rDNA were excised and purified by the phenol–chloroform method.

With amplified and purified 16S rDNA, a cloning process was performed using the vector pGem-T Easy (Promega, USA) with 50 µL of competent JM109 high-efficiency *E. coli* cells (Promega, USA) following the instructions provided by the manufacturer. Cloned cells were cultivated on plates of 1.5% LB–agar medium (in $g \cdot L^{-1}$: 10 tryptone, 10 NaCl, and 5 yeast extract; pH 7.0) with 100 $\mu g \cdot mL^{-1}$ ampicillin, 100 µL of 100 mM IPTG (Sigma-Aldrich, USA), and 20 µL of 50 $mg \cdot mL^{-1}$ X-Gal (Sigma-Aldrich, USA) and cultivated at 37 °C overnight. The colonies furthest away from their neighbors (all colonies on the plates had the same morphology) were selected (8 in total: 4 T6-OC and 4 T6-AC) and cultivated overnight in LB with 100 $\mu g \cdot mL^{-1}$ ampicillin. Plasmid DNA extraction was performed following a homemade lysozyme method. To verify the presence of the insert, digestions were carried out using an Anza 11 EcoR1 (Invitrogen) according to the supplier's protocol. Once verified, samples were sequenced at LANBAMA (National Laboratory of Biotechnology, San Luis Potosi, Mexico) in an Applied Biosystems 3130 Genetic Analyzer by the Sanger method using the pUC/M13 (Promega) primers. We obtained 16S rRNA gene sequences of 36 clones in total. After comparing these sequences with the GenBank database (Available online: www.ncbi.nlm.nih.gov/genbank/; May 2019 and September 2021) using the BLAST tool vs. 16S rRNA gene sequences [34], we reported only the sequences with an identity percentage greater than 95% (Table S2).

2.4. Two-Stage Oxidation of Pyrite

A two-stage chemical–bacterial FeS_2 oxidation assay was performed in Km medium (pH 2.0) using $BioFe^{3+}$ for the first stage and evaluating two independent chemical preoxidations at 30 and 90 °C. For both assays, the FeS_2 concentrate (10% w/v) was preoxidized

for 4 h with 4.1 g $Fe^{3+}{\cdot}L^{-1}$ added as $Fe_2(SO_4)_3{\cdot}7H_2O$ or with 4.1 g$\cdot L^{-1}$ of $BioFe^{3+}$ previously obtained from the T6 bacteria, as described below.

An inoculum of 2 × 10^7 cells$\cdot mL^{-1}$ from the T6 solution was transferred to a Km medium supplemented with 14 and 20 g$\cdot L^{-1}$ $Fe_2SO_4{\cdot}7H_2O$ to produce Fe^{3+} ($BioFe^{3+}$) ions. Next, the solution with $BioFe^{3+}$ was filtered through polycarbonate filters with a 0.22 µm pore size and analyzed for Fe^{2+} concentration by potentiostatic titration. Moreover, the accumulated specific productivity of Fe^{3+} ions ($\overline{q}_{Fe^{3+}}$) was calculated according to Saavedra et al. [29]:

$$\overline{q}_{Fe^{3+}} = \frac{\Delta\left[Fe^{3+}\right]}{\Delta[\#\,Cell] \times \Delta t} \quad (4)$$

where $[Fe^{3+}]$ is the concentration in grams per liter, t is the time in hours, and [# Cell] is the density of active live cells in cells per liter.

Once the $BioFe^{3+}$ had been obtained, the FeS_2 concentrate (10% *w*/*v*) was preoxidated with $BioFe^{3+}$ at 120 rpm under magnetic agitation at 30 and 90 °C, in triplicate; the same conditions were used for preoxidation of FeS_2 with Fe^{3+} at 30 and 90 °C.

The second stage was that of bio-oxidation. After the FeS_2 had been preoxidated with $BioFe^{3+}$ at 30 and 90 °C, the supernatant of each assay was decanted and replaced with fresh Km medium with an inoculum of the T6-AC culture (2 × 10^6 cells$\cdot mL^{-1}$). All the trials were incubated at 30 °C and 120 rpm, in triplicate.

During preoxidation as well as during bio-oxidation, the pH, redox potential, and concentration of soluble Fe^{3+} and sulfate ($SO_4{}^{2-}$) were monitored. On the last day of the bio-oxidation stage, samples of the remaining concentrate were analyzed by SEM-EDAX for the dissolution of Au and Ag by cyanidation.

Cyanidation of the concentrate was performed by the roll-bottle procedure using concentrate (10%w solid slurry) and 3 g$\cdot L^{-1}$ NaCN as the leaching or extractant agent. The pH was adjusted to 10.5 to 11.0 and was maintained throughout the leaching tests. The mixture was stirred at room temperature for 4, 6, 24, 48, 72, and 96 h. After each leaching period, the pregnant solution was sampled; also, the residues were sampled, filtered, and dried after each leaching period. The Au and Ag content of the pregnant solutions and the residual concentrate was determined by atomic absorption spectrometry (AAS). Due to environmental regulations, cyanidation was not carried out in our laboratory but by the mining company (Chihuahua, Mexico).

2.5. Analytical Methods

The microbial concentration (density of live active cells) was obtained by Neubauer chamber counting after centrifugation (21,000× *g* per 1.5 min). The solutions were analyzed after vacuum filtration for pH and redox potential (ORP) (Thermo Electron pH meter), total Fe by atomic absorption spectrometry (AAS) (Perkin Elmer 3100), Fe^{2+} (titration with 0.01 N $K_2Cr_2O_7$), and Fe^{3+} ions (difference between total Fe and Fe^{2+} concentrations). The concentration of $SO_4{}^{2-}$ was measured by the colorimetric method with barium chloride (8%) in acidic media and analyzed with a UV-vis spectrophotometer (Thermo Scientific, Waltham, MA, USA) at 420 nm. A scanning electrode microscope (SEM) (Phillips XL-30) coupled with an energy-dispersive Si(Li) detector (EDAX DX4) was used for particle analyses after bioleaching assays at a nominal resolution of 3.5 nm up to 30 kV.

3. Results and Discussion

3.1. Strains of A. ferrooxidans Identified in the Remnant Solution T6

The microorganisms were genetically identified to describe the community in the remnant T6 solution. The results showed that the T6 solution contained a metapopulation composed of at least four strains of *A. ferrooxidans* (Figure 1), since (a) the 16S rRNA gene sequences obtained from three T6 samples (named T6-OC1, T6-OC2, and T6-OC4) and three sequences from the adapted cultures (T6-AC1, T6-AC3, and T6-AC4) showed 100% identity with *A. ferrooxidans* ATCC-23270 NR_074193.1 [40] and NR_041888.1 [28] and (b) T6-OC3

and T6-AC2 are only 99.33% and 99.10% identical, respectively, to the cited strain. Two clones from T6-OC (clones of T6-OC5) showed 100% identity with the DQ321746.1 strain of *A. ferrooxidans*.

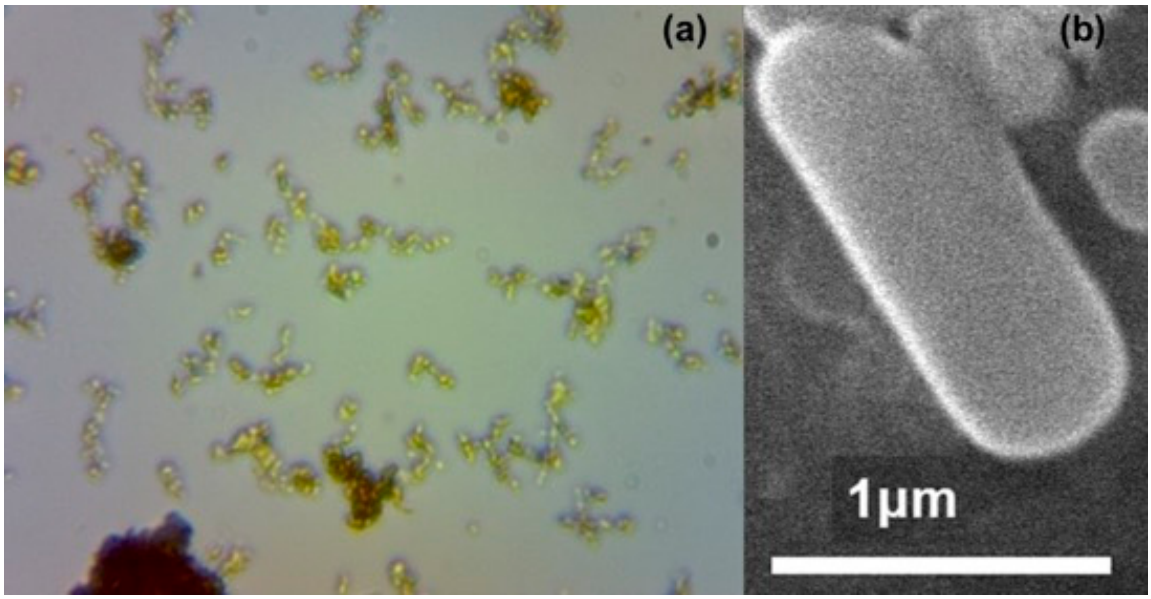

Figure 1. (**a**) Bacterial cells from the T6 remnant solution from a biohydrometallurgical process, observed under an optical microscope (40×). (**b**) An image obtained by SEM (20,000×) shows a single cell from T6.

A. ferrooxidans is a Gram-negative bacillus (rod-shaped) 1–1.5 µm in length and 0.5 µm in diameter that occurs as single cells or in pairs or chains but does not form endospores. The strains were cultivated as aerobic obligate acidophile chemilithoautotrophs, using molecular oxygen and ferric iron as electron acceptors for cultures without sulfur, or sulfur for cultures with S^0 or with FeS_2. Strains from both OC and AC cultures were at a pH between 1.4 and 2.0.

Sample T6-OC3 exhibited three nucleotide substitutions and Sample T6-AC2 had three different substitutions and one nucleotide addition, all within the highly conserved region of the 16S gene. These differences implied new wild strains of *Acidithiobacillus ferrooxidans* not yet described. Sequences of Samples T6-OC3 and T6-AC2 were reported to GenBank (https://www.ncbi.nlm.nih.gov/genbank/; 1 June 2021). The corresponding NCBI sequence numbers are MZ517251.1 and MZ517257.1, respectively.

A further study was performed with the obtained sequences according to Nuñez et al. [41]. *A. ferrooxidans* strains were found within two subclades (2A and 2B), represented mainly by seven strains (ATCC-23270, MCM-49, and Riv 11 for Subclade 2A; DSM-1927, VIR APRN1, HSS-3, and *A.* sp. SN108 for Subclade 2B). We performed an alignment of the sequences obtained in this work and the seven sequences that described Subclades 2A and 2B from the work of Nuñez et al. [41] (Figure 2), using the strain ATCC-19377 of *A. thiooxidans* as a differentiator control. Nucleotide substitutions on T6-OC3 can be seen in Positions 343, 419, and 429 (Figure 2). T6-AC2 substitutions occurred at Positions 233, 302, and 319 and a nucleotide addition was present at Position 191 (Figure 2). Other single nucleotide differences present in the strains that are representative of Subclades 2A and 2B [41] are also shown in the alignment in Figure 2, confirming that a single nucleotide change within the 16S gene indicates that a different strain has been found.

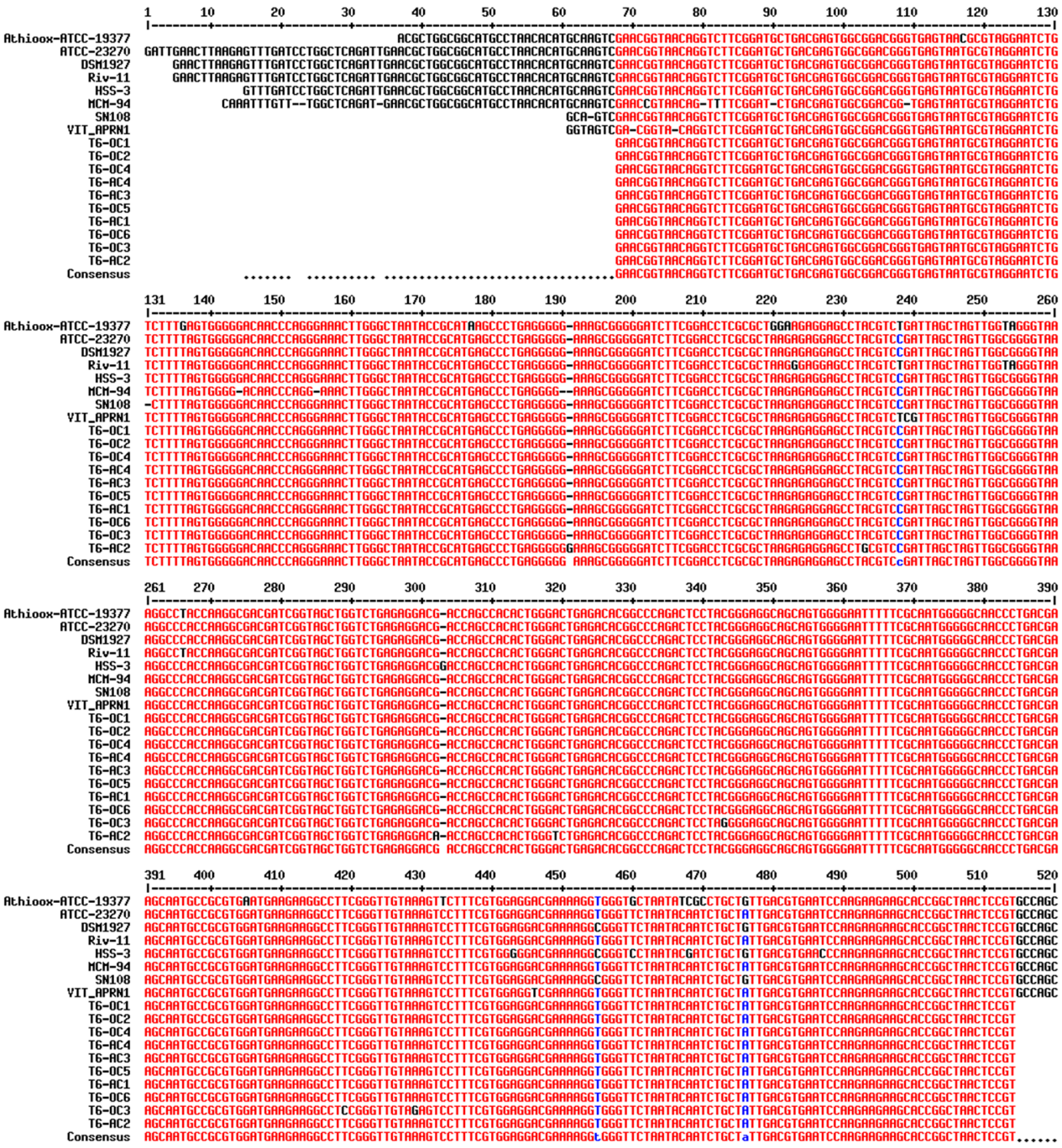

Figure 2. Alignment of the sequences obtained versus the sequences of representative strains for Subclades 2A and 2B from Nuñez et al. [41]. Red: consensus level of 95%; blue: consensus level of 50%. Created with MultAlin online software [42].

As Gevers [43] summarized, prokaryote species have diverse metabolisms and ecotypes, so the definition of species among bacteria has been debated for a long time. Differences in the genome of a bacterium can define different capacities in different individuals, despite being the same species. Thus, the four different strains identified after amplification of the sequence of *A. ferrooxidans* suggest the presence of a metapopulation [44], as they are four subpopulations that "occupy a minimally adaptive different zone" or, as Levins described, a "population of populations" [45]. Despite the term "metapopulation" having been conceived initially for macroorganisms, it has already been used for microorganisms, e.g., Keymer et al. [46], whose work proved that a metapopulation of bacteria emerges when they are inoculated into a habitat constituting different patches.

Moreover, the term "metapopulation" has been used in other microbial population studies, e.g., Mc Ginty et al. [47] and Goethert et al. [48]. In this work, we propose that a metapopulation of *A. ferrooxidans* is present in the solution T6 as the solution itself is a complex habitat containing several mineral particles to which bacterial biofilms adhere, comprising different patches within the same habitat. Pristas et al. [49] also showed that actual genomic analyses are indicative of pronounced genetic diversity within the *Acidithiobacillus* genus, especially within the *A. ferrooxidans* clade.

Even though further genomic analyses are required, we can assume that different populations from one single species composed of four strains are present in the communities T6-OC and T6-AC, providing a new example of the existence of a bacterial metapopulation.

After having been identified, the strains were cultivated as aerobic obligate acidophilous chemilithoautotrophs, using molecular oxygen and Fe^{3+} as the electron acceptors for cultures without sulfur, or sulfur for cultures with S^0 or with FeS_2. Strains from both the OC and AC cultures were at pH values between 1.4 and 2.0.

3.2. Bioferric Production by *A. ferrooxidans* Strains

The production of bioferric material by *A. ferrooxidans* strains was assayed to enhance the subsequent FeS_2 bio-oxidation, applying two-stage chemical-bacterial oxidation, since the strains of *A. ferrooxidans* from T6 (T6-OC) were already adapted to a high concentration of endogenous Fe^{2+} (Table 2), and Fe^{2+}-adapted cells may increase the volumetric productivity of Fe^{3+} [29], as was observed after our assays for the bioproduction of Fe^{3+} (or $BioFe^{3+}$) (see below). Moreover, the *A. ferrooxidans* strains from T6 were tolerant of Cu, Zn, Pb, and As (Table 2), as was previously reported [21,50,51]. Furthermore, Rawlings et al. [51] reported that total Fe concentrations of up to 20 $g{\cdot}L^{-1}$ have no inhibitory effect on the oxidizing activity of *A. ferrooxidans*.

Table 2. Certain characteristics of the remnant solution T6 and the precipitate formed at the bottom of the containers. Metal concentrations are given in grams per liter ($g{\cdot}L^{-1}$).

Solution	pH	Eh (mV)	Total Fe	Fe^{2+}	Cu	Zn	Pb	As	Biomass (Cells·mL^{-1})
T6	3.05	552	30.9	27	57	127	1.2	7.5	14×10^6
Precipitate composition	Jarosite, $KFe_3(SO_4)(OH)_6$ (83.7%); rozenite, $FeSO_4{\cdot}4H_2O$ (16.34%)								

The results of our assays for the bioproduction of Fe^{3+} ($BioFe^{3+}$) by *A. ferrooxidans* strains cultured at 30 °C showed that T6-OC generated >97.7% of $BioFe^{3+}$ after 56 h in the Km medium supplemented with two different initial Fe^{2+} concentrations (Table 3), while the pH remained constant (~2.1). However, with an initial Fe^{2+} concentration of 14 $g{\cdot}L^{-1}$, the redox potential increased to 800 mV, which favored FeS_2 (bio)oxidation [9].

Table 3. Concentration of Fe^{2+} oxidized and $BioFe^{3+}$ generated, percentage of $BioFe^{3+}$ generated, and specific productivity of Fe^{3+} ions ($\overline{q}_{Fe^{3+}}$) after 56 h, assayed in two initial Fe^{2+} concentrations.

Initial Fe^{2+} ($g{\cdot}L^{-1}$)	Final Fe^{2+} ($g{\cdot}L^{-1}$)	Final $BioFe^{3+}$ ($g{\cdot}L^{-1}$)	Final %$BioFe^{3+}$	$\overline{q}_{Fe^{3+}}$ (gFe^{3+} cel^{-1} h^{-1})
14	0.0	14.0	100	3.97×10^{-7}
20	0.5	19.53	97.7	3.86×10^{-7}

Therefore, we did not preadapt the *A. ferrooxidans* strains to progressively higher concentrations of Fe, as has been suggested [29], because we used a metapopulation that was already adapted to a high Fe concentration, as indicated by the results obtained from the remnant solution analyses (Table 2). Mousavi et al. [52] also used a native strain of *A. ferrooxidans* with 20.2 g Fe^{2+} per L, obtaining a maximum bio-oxidation rate of 1.2 $g{\cdot}L^{-1}{\cdot}h^{-1}$ after 70 h. The results showed that with autochthonous and already adapted

strains, the production of bioferric flocculant from an initial concentration of 14 and 20 g·L^{-1} of Fe^{2+} occurred relatively quickly (56 h) even at 30 °C (Table 2). Consequently, the specific Fe^{2+} bio-oxidation activity of the assayed *A. ferrooxidans* strains was high (Table 3). This reinforces the importance of using native species, which must be identified even down to the strain level, as Karavaiko et al. [28] suggested.

Furthermore, the density of active cells increased from 2×10^6 to 9×10^6 cells·mL^{-1} (average after centrifugation of the culture sample) at a final Fe^{3+} concentration of up to 19.5 g·L^{-1}, while the specific Fe^{2+} bio-oxidation activity ($\overline{q}_{Fe^{3+}}$) of *A. ferrooxidans* strains was relatively high (Table 2) compared with that found in other studies; e.g., Saavedra et al. [29] reported a $\overline{q}_{Fe^{3+}}$ of 1.75×10^{-8} g Fe^{3+} cells^{-1} h^{-1} for cells adapted to 18 g Fe^{3+}·L^{-1}. These authors obtained planktonic cells covered with EPS, demonstrating that *A. ferrooxidans* has a greater EPS content on its cell surfaces, which enhances its tolerance to high Fe^{3+} ion concentrations. Developing as biofilms (Figure 1), cells of *A. ferrooxidans* can tolerate higher concentrations of Fe^{3+} [29,53] and, in adapted cells forming biofilms, EPS-complexed Fe^{3+} by electrostatic interactions may increase the FeS_2 dissolution rate [54].

3.3. Chemical Preoxidation Followed by Biological Oxidation of Pyrite

3.3.1. Chemical Preoxidation of Pyrite

The strains of *A. ferrooxidans* from the T6-OC remnant solution (Table 1) assisted the production of $BioFe^{3+}$. Following this, the FeS_2 was chemically preoxidized for 4 h at 30 °C with the $BioFe^{3+}$ at 4 g·L^{-1}, and with 4 g/L of Fe^{3+} added as $Fe_2(SO_4)_3$·$7H_2O$ as a comparison.

The FeS_2 preoxidation exposing the FeS_2 concentrate to $BioFe^{3+}$ or Fe^{3+} at 90 °C ($TBioFe^{3+}$ or TFe^{3+}, respectively), resulted in a higher oxidation rate that than at 30 °C, as indicated by the lower pH values and redox potential after 4 h (Figure 3a,c), as well as the high sulfate production and Fe^{3+} consumption (Figure 3b,d). These results were expected as the catalytic effect of temperature also favors Fe^{3+} precipitation [19,55,56]. Moreover, higher sulfate production and Fe^{3+} consumption in the $TBioFe^{3+}$ trials can be noted.

During preoxidation of the FeS_2 concentrate at 30 °C, the pH, the redox potential, and the concentration of sulfates and Fe^{3+} changed to a lesser extent than during preoxidiation at 90 °C, particularly in batches with Fe^{3+}. In other words, the use of $BioFe^{3+}$ seems to be more effective at both 30 and 90 °C than the use of commercial salt. For example, the concentration of total Fe in the solution was up to 50% after preoxidation with the Fe^{3+} salt, but up to 58.5% with $BioFe^{3+}$; the use of Fe^{3+} salt also generated more sulfate precipitates [56] than the use of $BioFe^{3+}$ (Figure 4), according to the following reaction [14]:

$$FeS_2 + 7Fe_2(SO_4)_3 + 8H_2O \rightarrow 15FeSO_4 + 8H_2SO_4 \quad (5)$$

The formation of jarosite precipitates hinders FeS_2 oxidation [12]. Because of greater jarosite formation after preoxidation with Fe^{3+} salt, we only carried out the bio-oxidation stage of the pretreated FeS_2 concentrate with $BioFe^{3+}$.

3.3.2. Biological Oxidation of Pyrite Concentrate

At the end of the preoxidation stage, the FeS_2 concentrate from each experimental batch was exposed to microorganisms from T6 to initiate the second stage of the process, namely bio-oxidation of the pretreated FeS_2 concentrate. Figure 3 summarizes the Fe^{3+} and the sulfate concentration, and the pH and redox potential of the media during both stages of oxidation of the FeS_2 concentrate.

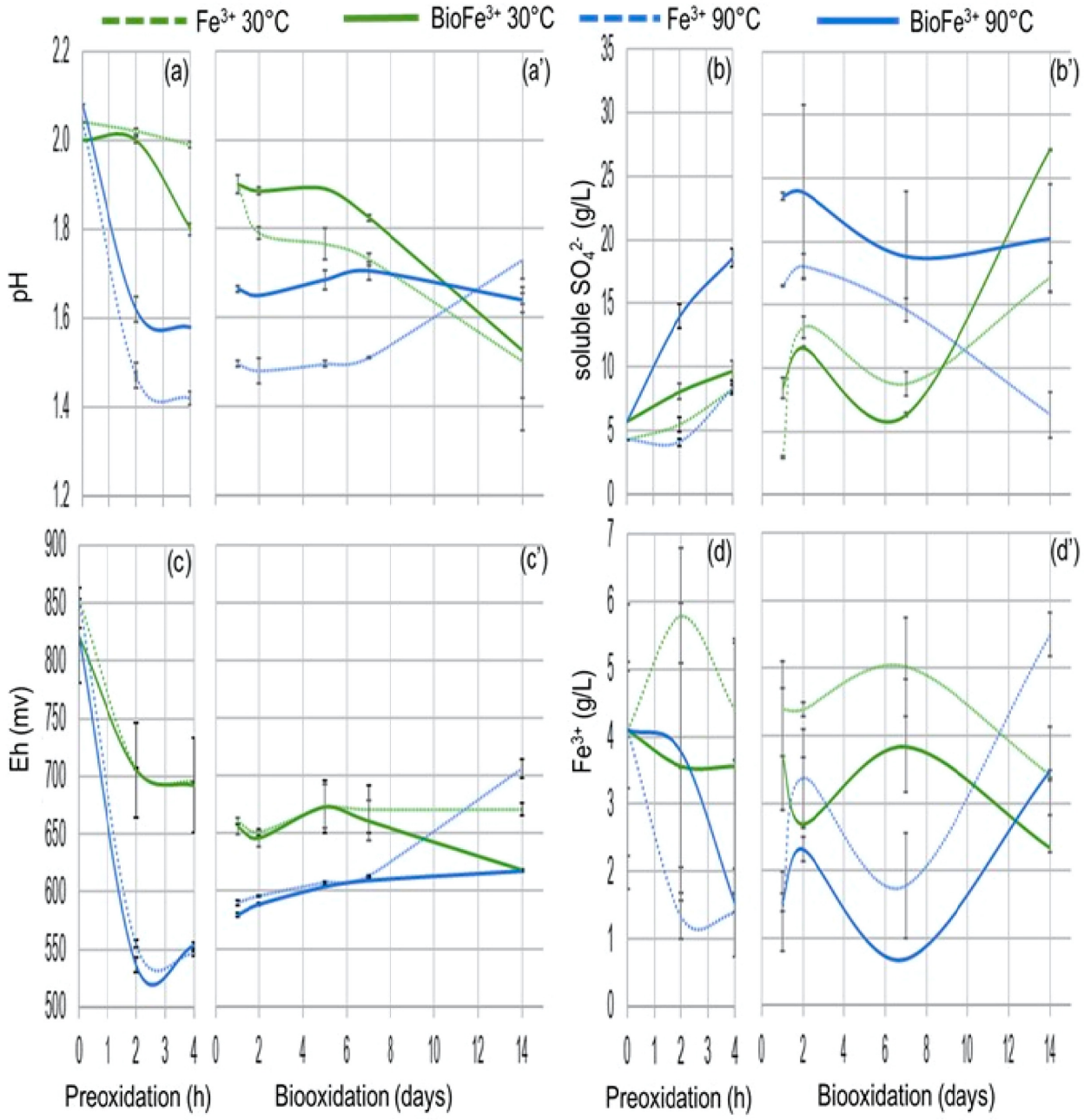

Figure 3. Results of pH, sulfate concentration, redox potential, and ferric ion concentration during: (**a**–**d**) FeS_2 concentrate (10% *w*/*v*) preoxidation with bioferric ($BioFe^{3+}$) (solid lines) or with ferric sulfate, Fe^{3+} (dotted lines) at 30 °C (green lines) or 90 °C (blue lines) and during (**a'**–**d'**) bio-oxidation of the preoxidized FeS_2 concentrate at 30 and 90 °C with $BioFe^{3+}$.

The evolution of pH, sulfates, and the Fe^{3+} concentration during this second stage of the process (i.e., biological oxidation) are shown in Figure 3. Fe^{3+} was regenerated by the active biomass of the inoculated *A. ferrooxidans* strains Equation (2) in the batches with the preoxidized FeS_2 concentrate at 90 °C, indicated by the increased concentration of this ion during the first 2 days of the second stage (Figure 3d). From days 2 to 7, oxidation of the FeS_2 concentrate proceeded as the Fe^{3+} consumption indicated, due to the ferric oxidation of FeS_2 Equation (1) but lower acidity production (Figure 3a) and sulfate solubilization (Figure 3b) were recorded. From days 7 to 14, the Fe^{3+} was regenerated by *A. ferrooxidans*. Notably, the production of soluble sulfate ceased; its concentration even decreased, especially in trials where the FeS_2 concentrate was preoxidized with TFe^{3+} (Figure 3b). This may be because of sulfate precipitation due to acid consumption:

with increased pH and in the presence of iron, the concentration of alkaline sulfates increases [55,56]. The formation of jarosite precipitate hinders FeS_2 (bio)oxidation [12].

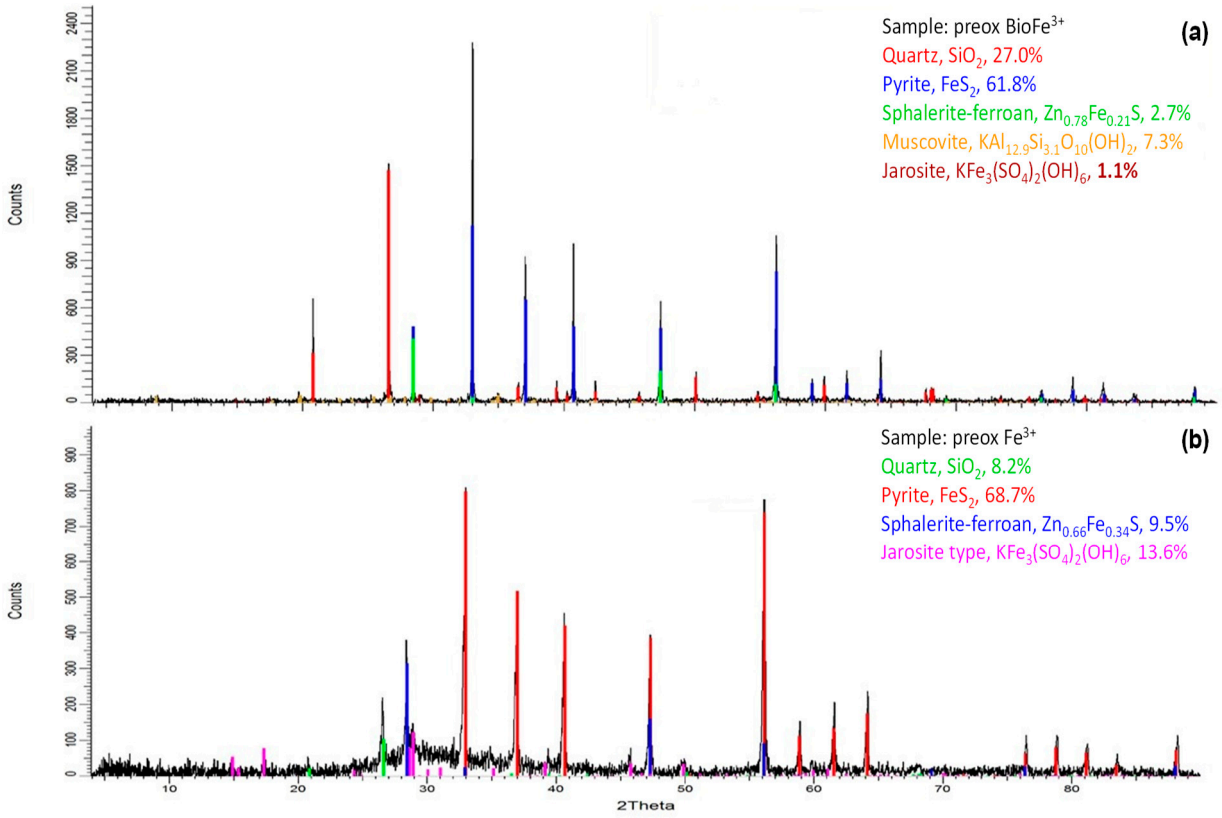

Figure 4. XRD results of precipitates obtained after preoxidation of the FeS_2 concentrate with (**a**) BioFe^{3+} and (**b**) Fe^{3+} at 30 °C. Note: Different color codes were used in (**a**,**b**) for the minerals; e.g., FeS_2 is shown in blue in (**a**) but in red in (**b**).

The opposite occurred after bio-oxidation of the preoxidized FeS_2 concentrate at 30 °C, in which the ferric oxidation of the FeS_2 remained Equation (1) for the first 2 days, followed by the regeneration of Fe^{3+} Equation (2) on days 2 to 7 and its subsequent use as an oxidizing agent Equation (2) during days 7 to 14, which resulted in greater production of sulfate and acidity Equation (3). There was a notable increase in the sulfate concentration (up to 324%), as well as a constant decrease in pH when using the concentrate preoxidized with BioFe^{3+} (Figure 3a).

The accumulated specific productivity of Fe^{3+} ions, $\overline{q}_{Fe^{3+}}$, shows a marked difference in the specific bio-oxidation activity of *A. ferrooxidans* on the preoxidized FeS_2 concentrate (Figure 5). BioFe^{3+} actively oxidized the remaining preoxidized FeS_2 concentrate at 30 °C for the first 24 h, followed by BioFe^{3+} regeneration by the increasing biomass of *A. ferrooxidans* strains (24 to 48 h), and its consumption as an oxidant agent, until the $\overline{q}_{Fe^{3+}}$ remained constant (168 and 336 h), confirming that the cells had adapted to the process [29]. In contrast, using the FeS_2 concentrate preoxidized at 90 °C (TBioFe^{3+}), the BioFe^{3+} was regenerated but gradually accumulated until it precipitated as late as day 14 (336 h).

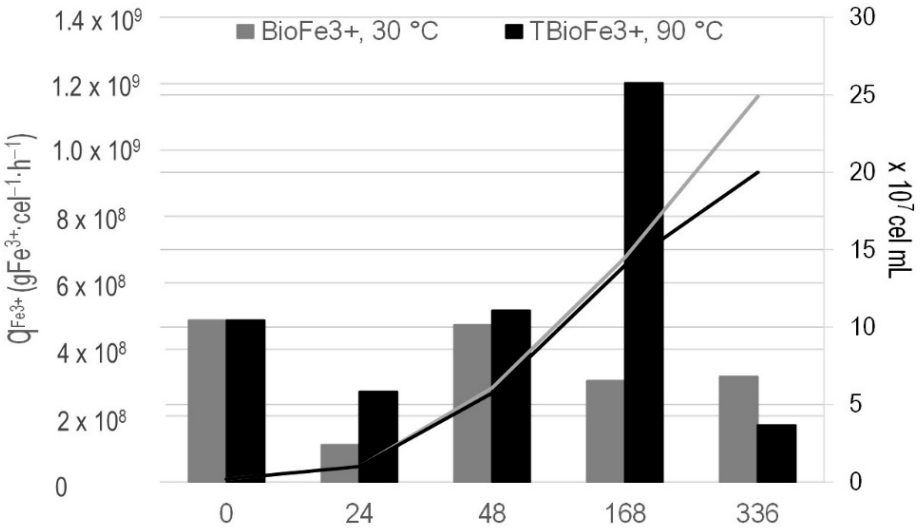

Figure 5. Accumulated specific productivity of Fe^{3+} ions ($\overline{q}_{Fe^{3+}}$) and biomass density after 336 h of bio-oxidation using the T6 community and the FeS_2 concentrate previously preoxidized with $BioFe^{3+}$ at 30 or 90 °C.

Thus, $BioFe^{3+}$ seems to be an important booster for FeS_2 bio-oxidation. In the presence of FeS_2, the EPS produced by *A. ferrooxidans* was mainly composed of neutral sugars, C12–20 saturated fatty acids, some glucuronic acid residues, and complexed Fe^{3+} ions [57]; therefore, it may enhance the bioleaching process.

Finally, the bio-oxidation of the preoxidized FeS_2 concentrate with $BioFe^{3+}$ at 30 °C triggered the release of Au particles from day 14 onwards (Figure 6a,b); these trials were maintained for a further 35 days (49 days in total). Non-occluded Au particles could be observed after 21 days (Figure 6c), but mainly after 28 days (Figure 6e,f). However, Ag particles were only observed after 49 days (Figure 6g,h). Notably, neither sulfates nor elemental sulfur were detected on the surface of the FeS_2 particles (Figure 6).

3.3.3. Gold and Silver Extraction

Samples of the FeS2 concentrate obtained after 21, 25, and 35 days were treated to cyanide leaching, to extract the Au and Ag at the end of chemical–bacterial oxidation at 30 °C. The Au and Ag recovery are presented in Table 4, and the last column reports the Au and Ag by cyanide leaching of the concentrate. The maximum Au and Ag extraction rates were after 96 h of cyanidation, the extraction percentages were up to 30.5% Au and 57.9% Ag after 21 days of bio-oxidation.

Table 4. Analyses and extraction of Au and Ag from the FeS_2 concentrate at the end of chemical–bacterial oxidation. Data show the maximum value reached after 72 to 96 h of agitation leaching using NaCN as the extractant.

Oxidation Duration, Day	Oxidation Residue [1]		Cyanidation Residue		Pregnant Solution		Extraction	
	Au ($g \cdot T^{-1}$)	Ag ($g \cdot T^{-1}$)	Au ($g \cdot T^{-1}$)	Ag ($g \cdot T^{-1}$)	Au ($mg \cdot L^{-1}$)	Ag ($mg \cdot L^{-1}$)	Au (%)	Ag (%)
21	2.89	75	2.59	32	0.11	4.18	30.52	57.97
25	2.90	73	2.65	35	0.09	4.05	27.17	55.27
35	2.96	74	2.65	34	0.09	3.75	27.09	54.42

[1] Au and Ag in the original concentrate before chemical–bacterial oxidation.

These results have been communicated to the mining company in North-west Mexico to optimize the process of exploiting their waste material and obtaining Au and Ag, ideally through the two-step process assayed in this work using local strains of *A. ferrooxidans* from their T6 remnant solution.

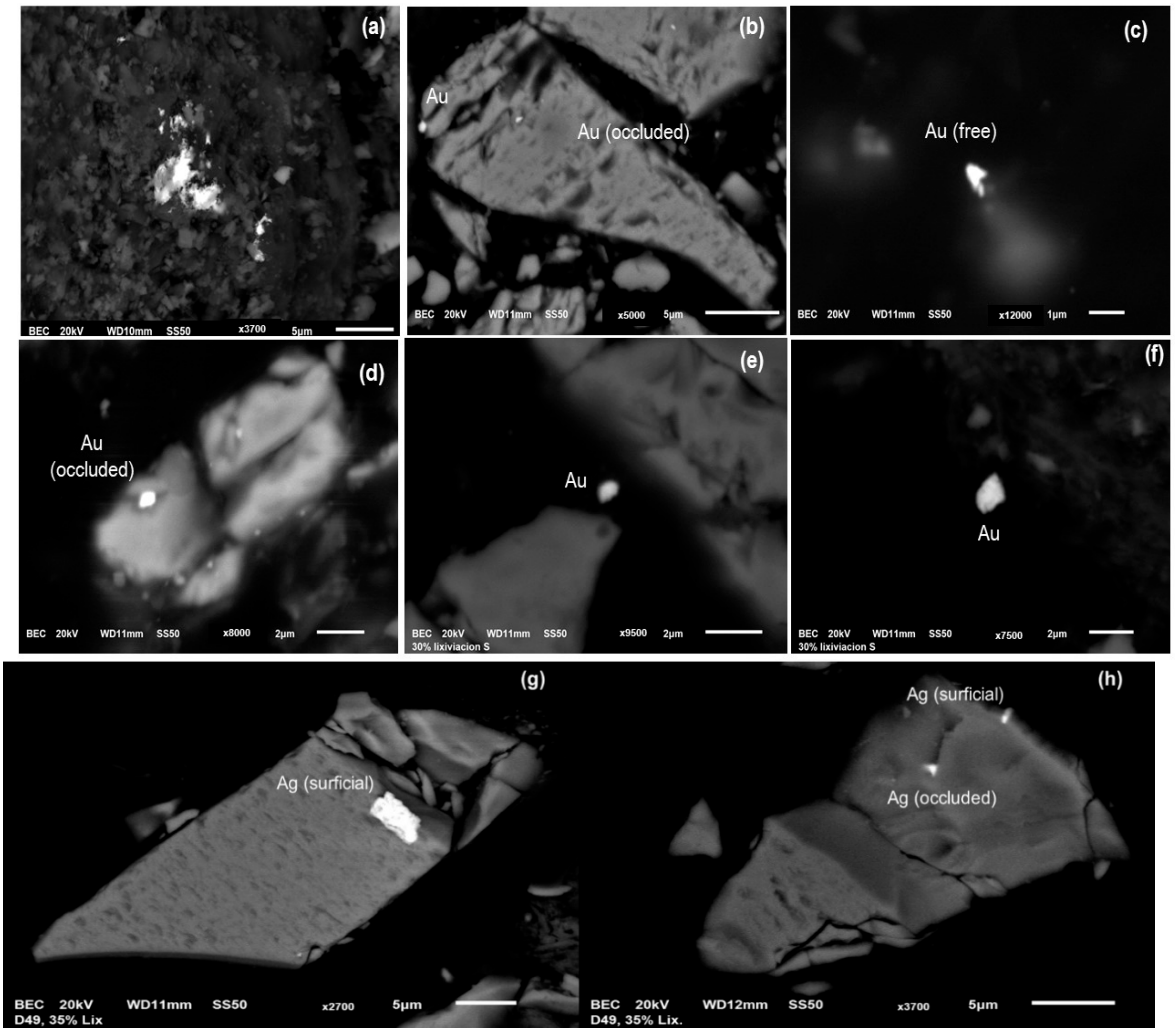

Figure 6. Images obtained by SEM of bio-oxidated FeS_2 particles after 14 (**a**,**b**), 21 (**c**,**d**), and 28 (**e**,**f**) days (previously preoxidized with bioferric flocculant at 30 °C), in which the gold particles (Au) stand out. (**b**) FeS_2 with Au occlusions (<1 µm), one at the edge (**left**) and the other within the particle (**center**); (**c**) Au in the free state; (**d**) Au entrapped in FeS_2; (**e**,**f**) Au in free state after 30% oxidation of the FeS_2 concentrate. (**g**,**h**) After 49 days of the assays, partially occluded Ag particles were observed with a size of 5 µm (**g**) or less (**h**). For SEM-EDX analysis, samples were prepared by resin mounting with mirror-finish surface exposure.

4. Conclusions

In this work, a successful standardized method was described for isolating bacteria and obtaining functional genomic material for further experiments such as RT-PCR and cloning protocols from a complex and highly acidic solution. We also present a novel pair of primers to amplify a small region of the 16S gene that contains the greatest intraspecies diversity. The original community from a remnant solution (T6-OC) maintained a similar composition of *A. ferrooxidans* strains after the adaptation process (T6-AC). Thus, the T6 solution with a *A. ferrooxidans* metapopulation that is already adapted to FeS_2 permits bio-oxidation activity, which is reflected in the accumulated specific productivity of the Fe^{3+} ions ($\overline{q}_{Fe^{3+}}$). As in other studies, the tolerance of this species to $\geq$20 g Fe·L^{-1} was again demonstrated. The BioFe^{3+} was obtained in a relatively short time (56 h) and used for FeS_2 preoxidation at 30 °C, allowing the lower presence of passivation compounds and therefore detection of free Au and Ag particles after biooxidation of the preoxidized FeS_2. The wild strains found in both the T6-OC and T6-AC cultures may explain the improved bio-oxidation capacity and accelerated BioFe^{3+} production, but further genomic and bioox-

idation assays should be carried out to confirm this. The discovery of a metapopulation of four strains of *A. ferrooxidans* sharing minimally different niches in T6 was shown. These findings should be considered by the mining company to exploit its mine tailings using its autochthonous metapopulation of *A. ferrooxidans* as sources of free particles of Au and Ag. Of course, it will be necessary to accelerate the two-stage process and evaluate it in terms of its costs and benefits.

Supplementary Materials: The following are available online at https://www.mdpi.com/article/10.3390/mining1030021/s1, Table S1. Nucleotide BLAST summary. Results with F63 and R533 primers against proposed bacterial genera. Table S2. Sequences obtained from the original and the adapted communities after cloning process.

Author Contributions: Conceptualization, A.E.J.-P. and J.V.G.-M.; data curation, A.E.J.-P., E.F.A.-S. and A.H.-S.; formal analysis, A.E.J.-P., E.F.A.-S., A.H.-S. and J.V.G.-M.; funding acquisition, J.V.G.-M.; investigation, A.E.J.-P., E.F.A.-S., A.H.-S. and J.V.G.-M.; methodology, A.E.J.-P., E.F.A.-S., A.H.-S. and J.V.G.-M.; project administration, J.V.G.-M.; writing—original draft, A.E.J.-P., E.F.A.-S., A.H.-S. and J.V.G.-M.; writing—review & editing, A.E.J.-P., and J.V.G.-M. All authors have read and agreed to the published version of the manuscript.

Funding: No funder had any role in the analyses or interpretation of data, in the writing of the manuscript, or in the decision to publish the results.

Data Availability Statement: Not applicable.

Acknowledgments: The authors thank I.A. Manuel, A. Sanchez Olvera, I.A. J. Salvador Zaragoza, and Marizel Astello for their support in carrying out this work. Special thanks are due to Francisco Galindo for the SEM and ESEM analyses, and to Rosa Linda Tovar for the DRX analyses.

Conflicts of Interest: The authors declare no conflict of interest.

References

1. Gorain, B.K.; Kondos, P.D.; Lakshmanan, V.I. Innovations in gold and silver processing. In *Innovative Process Development in Metallurgical Industry*; Lakshmanan, V., Roy, R., Ramachandran, V., Eds.; Springer: Cham, Switzerland, 2016; pp. 393–428. [CrossRef]
2. Jafari, M.; Abdollahi, H.; Shafaei, S.Z.; Gharabaghi, M.; Jafari, H.; Akcil, A.; Panda, S. Acidophilic bioleaching: A review on the process and effect of organic-inorganic reagents and materials on its efficiency. *Minrt. Proces. Extr. Metall. Rev.* **2018**, *40*, 87. [CrossRef]
3. Brune, K.; Bayer, T. Engineering microbial consortia to enhance biomining and bioremediation. *Front. Microbiol.* **2012**, *3*, 203. [CrossRef]
4. He, J.; Kappler, A. Recovery of precious metals from waste streams. *Microbial Biotechnol.* **2017**, *10*, 1194. [CrossRef] [PubMed]
5. Siezen, R.; Wilson, G. Bioleaching genomics. *Microbial Biotechnol.* **2009**, *2*, 297. [CrossRef] [PubMed]
6. Evangelou, V.; Zhang, Y. A review: Pyrite oxidation mechanisms and acid mine drainage prevention. *Crit. Rev. Environ. Sci. Technol.* **1995**, *25*, 141. [CrossRef]
7. Tao, H.; Dongwei, L. Presentation on mechanisms and applications of chalcopyrite and pyrite bioleaching in biohydrometallurgy—A presentation. *Biotechnol. Rep.* **2014**, *4*, 107. [CrossRef]
8. Sánchez-Andrea, I.; Rodríguez, N.; Amils, R.; Sanz, J. Microbial diversity in anaerobic sediments at Río Tinto, a naturally acidic environment with a high heavy metal content. *App. Environ. Microbiol.* **2011**, *77*, 6085. [CrossRef]
9. Sun, H.; Chen, M.; Zou, L.; Shu, R.; Ruan, R. Study of kinetics of pyrite oxidation under controlled redox potential. *Hydrometallurgy* **2015**, *155*, 13. [CrossRef]
10. Asamoah, R.K. Specific refractory gold flotation and bio-oxidation products: Research overview. *Minerals* **2021**, *11*, 93. [CrossRef]
11. Ghassa, S.; Noaparast, M.; Shafaei, S.Z.; Abdollahi, H.; Gharabaghi, M.; Boruomand, Z. A study on the zinc sulfide dissolution kinetics with biological and chemical ferric reagents. *Hydrometallurgy* **2017**, *171*, 362. [CrossRef]
12. Wang, G.; Xie, S.; Liu, X.; Wu, Y.; Liu, Y.; Zeng, T. Bio-oxidation of a high-sulfur and high-arsenic refractory gold concentrate using a two-stage process. *Miner. Eng.* **2018**, *120*, 94. [CrossRef]
13. Fomchenko, N.Y.V.; Muravyov, M.I.; Kondrat'eva, T.F. Two-stage bacterial-chemical oxidation of refractory gold-bearing sulfidic concentrates. *Hydrometallurgy* **2010**, *101*, 28. [CrossRef]
14. Fomchenko, N.; Muravyov, M. Sequential bioleaching of pyritic tailings and ferric leaching of nonferrous slags as a method for metal recovery from mining and metallurgical wastes. *Minerals* **2020**, *10*, 1097. [CrossRef]
15. Kaksonen, A.H.; Mudunuru, B.M.; Hackl, R. The role of microorganisms in gold processing and recovery—A review. *Hydrometallurgy* **2014**, *142*, 70–83. [CrossRef]

16. Li, Q.; Li, D.; Qian, F. Preoxidation of high-sulfur and high-arsenic refractory gold concentrate by ozone and ferric ions in acidic media. *Hydrometallurgy* **2009**, *97*, 61–66. [CrossRef]
17. Muravyov, M.I.; Bulaev, A.G. Two-step oxidation of a refractory gold-bearing sulfidic concentrate and the effect of organic nutrients on its biooxidation. *Miner. Eng.* **2013**, *45*, 108–114. [CrossRef]
18. Zheng, Y.; Wei, D.; Liu, W.; Duan, H.; Zhou, S. One novel two-step bio-oxidation pretreatment of arsenic-containing gold-bearing concentrate. *Int. J. Electrochem. Sci.* **2018**, *13*, 5983–5994. [CrossRef]
19. Steijns, M.; Derks, F.; Verloop, A.; Mars, P. The mechanism of the catalytic oxidation of hydrogen sulfide: II. Kinetics and mechanism of hydrogen sulfide oxidation catalyzed by sulfur. *J. Catal.* **1976**, *42*, 87–95. [CrossRef]
20. Fowler, T.A.; Holmes, P.R.; Crundwell, F. On the kinetics and mechanism of the dissolution of pyrite in the presence of *Thiobacillus ferrooxidans*. *Hydrometallurgy* **2001**, *59*, 257. [CrossRef]
21. Rawlings, D. Characteristics and adaptability of iron- and sulfur-oxidizing microorganisms used for the recovery of metals from minerals and their concentrates. *Microb. Cell Fact.* **2005**, *4*, 13. [CrossRef]
22. Rao, S.; Muyinda, N.; De Baets, B. Stability analysis of the coexistence equilibrium of a balanced metapopulation model. *Nat. Sci. Rep.* **2021**, *11*, 14084. [CrossRef]
23. Kunin, V.; He, S.; Warnecke, F.; Peterson, S.B.; Garcia-Martin, H.; Haynes, M.; Ivanova, N.; Blackall, L.L.; Breitbart, M.; Rohwer, F.; et al. Bacterial metapopulation adapts locally to phage predation despite global dispersal. *Genome Res.* **2008**, *18*, 293–297. [CrossRef] [PubMed]
24. Palacios, C.; Zettler, E.; Amils, R.; Amaral-Zettler, L. Contrasting microbial community assembly hypotheses: A reconciling tale from the Río Tinto. *PLoS ONE* **2008**, *3*, e3853. [CrossRef] [PubMed]
25. Mostowy, R.; Croucher, N.J.; Andam, C.P.; Corander, J.; Hanage, W.P.; Marttinen, P. Efficient inference of recent and ancestral recombination within bacterial populations. *Mol. Biol. Evol.* **2017**, *34*, 1167–1182. [CrossRef]
26. Sipola, A.; Marttinen, P.; Corander, J.; Berger, B. Bacmeta: Simulator for genomic evolution in bacterial metapopulations. *Bioinformatics* **2018**, *34*, 2308–2310. [CrossRef] [PubMed]
27. Zhang, X.; Feng, X.; Tao, J.; Ma, L.; Xiao, Y.; Liang, Y.; Liu, X.; Yin, H. Comparative genomics of the extreme acidophile *Acidithiobacillus thiooxidans* reveals intraspecific divergence and niche adaptation. *Int. J. Mol. Sci.* **2016**, *17*, 1355. [CrossRef]
28. Karavaiko, G.I.; Turova, T.P.; Kondrat'eva, T.F.; Lysenko, A.M.; Kolganova, T.V.; Ageeva, S.N.; Muntyan, L.N.; Pivovarova, T.A. Phylogenetic heterogeneity of the species *Acidithiobacillus ferrooxidans*. *Int. J. Syst. Evol. Microbiol.* **2003**, *53*, 113. [CrossRef]
29. Saavedra, A.; Aguirre, P.; Gentina, J.C. Climbing the hill: The implications of ferrous iron pulse adaptation on biooxidation by *Acidithiobacillus ferrooxidans*. *Hydrometallurgy* **2020**, *197*, 105485. [CrossRef]
30. Nemati, M.; Harrison, S.T.L. Effects of solid particles on thermophilic bioleaching of sulphide minerals. In *Biohydrometallurgy and the Environment*; Toward the Mining of the 21st Century-Part A; Amils, R., Ballester, A., Eds.; Elsevier: Amsterdam, The Netherland, 1999; pp. 473–482. [CrossRef]
31. Callender, K.; Roy, S.; Khasa, D.; Whyte, L.; Greer, C. Actinorhizal alder phytostabilization alters microbial community dynamics in gold mine waste rock from Northern Quebec: A greenhouse study. *PLoS ONE* **2016**, *11*, e0150181. [CrossRef]
32. Mesa, V.; Gallego, J.; González-Gil, R.; Lauga, B.; Sánchez, J.; Méndez-García, C.; Peláez, A. Bacterial, Archaeal, and Eukaryotic diversity across distinct microhabitats in an acid mine drainage. *Front. Microbiol.* **2017**, *8*, 1756. [CrossRef] [PubMed]
33. Marchesi, J.; Sato, T.; Weightman, A.; Martin, T.; Fry, J.; Hiom, S.; Wade, W. Design and evaluation of useful bacterium-specific PCR primers that amplify genes coding for bacterial 16S rRNA. *Appl. Environ. Microbiol.* **1998**, *6*, 795. [CrossRef] [PubMed]
34. Altschul, S.; Madden, T.; Schäffer, A.; Zhang, J.; Zhang, Z.; Miller, W.; Lipman, D. Gapped BLAST and PSI-BLAST: A new generation of protein database search programs. *Nucleic Acids Res.* **1997**, *25*, 3389–3402. [CrossRef]
35. Allen, H.K.; Bayles, D.O.; Looft, T.; Trachsel, J.; Bass, B.E.; Alt, D.P.; Bearson, S.M.D.; Nicholson, T.; Casey, T.A. Pipeline for amplifying and analyzing amplicons of the V1-V3 region of the 16S rRNA gene. *BMC Res. Notes* **2016**, 380. [CrossRef]
36. Scholss, P.D. The effects of alignment quality, distance calculation method, sequence filtering, and region on the analysis of 16S rRNA gene-based studies. *PLoS Comput. Biol.* **2010**, *6*, e1000844. [CrossRef]
37. Coenye, T.; Vandamme, P. Intragenomic heterogeneity between multiple 16S ribosomal RNA operons in sequenced bacterial genomes. *FEMS Microbiol. Lett.* **2003**, *228*, 45. [CrossRef]
38. Baker, G.C.; Smith, J.J.; Cowan, D.A. Review and re-analysis of domain-specific 16S primers. *J. Microbiol. Meth.* **2003**, *55*, 541. [CrossRef] [PubMed]
39. Wang, Y.; Qian, P.Y. Conservative fragments in bacterial 16S rRNA genes and primer design ribosomal DNA amplicons in metagenomics studies. *PLoS ONE* **2009**, *4*, e7401. [CrossRef]
40. Valdés, J.; Pedroso, I.; Quatrini, R.; Dodson, R.J.; Tettelin, H.; Blake, R.; Eisen, J.A.; Holmes, D.S. *Acidithiobacillus ferrooxidans* metabolism: From genome sequence to industrial applications. *BMC Genom.* **2008**, *9*, 597. [CrossRef] [PubMed]
41. Nuñez, H.; Moya-Beltrán, A.; Covarrubias, P.C.; Issotta, F.; Cárdenas, J.P.; González, M.; Atavales, J.; Acuña, L.G.; Johnson, D.B.; Quatrini, R. Molecular systematics of the genus *Acidithiobacillus*: Insights into the phylogenetic structure and diversification of the taxon. *Front. Microbiol.* **2017**, *8*, 30. [CrossRef]
42. Corpet, F. Multiple sequence alignment with hierarchical clustering. *Nucleic Acids Res.* **1988**, *16*, 10881. [CrossRef]
43. Gevers, D.; Cohan, F.M.; Lawrence, J.G.; Spratt, B.G.; Coenye, T.; Feil, E.J.; Stackebrandt, E.; Van de Peer, Y.; Vandamme, P.; Thompson, F.L.; et al. Opinion: Re-evaluating prokaryotic species. *Nat. Rev. Microbiol.* **2005**, *3*, 733. [CrossRef]

44. Achtman, M.; Wagner, M. Microbial diversity and the genetic nature of microbial species. *Nat. Rev. Microbiol.* **2008**, *6*, 431–440. [CrossRef]
45. Levins, R. Some demographic and genetic consequences of environmental heterogeneity for biological control. *Bull. Entomol. Soc. Am.* **1969**, *15*, 237. [CrossRef]
46. Keymer, J.E.; Galajda, P.; Muldoon, C.; Park, S.; Austin, R.H. Bacterial metapopulations in nanofabricated landscapes. *Proc. Natl. Acad. Sci. USA* **2006**, *103*, 17290–17295. [CrossRef] [PubMed]
47. Mc Ginty, S.E.; Rankin, D.J.; Brown, S.P. Horizontal gene transfer and the evolution of bacterial cooperation. *Evolution* **2010**, *65*, 21. [CrossRef]
48. Goethert, H.K.; Saviet, B.; Telford III, S.R. Metapopulation structure for perpetuation of *Francisella tularensis tularensis*. *BMC Microbiol.* **2009**, *9*, 147. [CrossRef] [PubMed]
49. Pristas, P.; Kiskova, J.; Timkova, I.; Malinicova, L.; Luptakova, A.; Kusnierova, M.; Sedlakova-Kadukova, J. Genetic variability in *Acidithiobacillus* spp. -A working horse of environmental biotechnologies. *Nova Biotechnol. Chim.* **2018**, *17*, 125. [CrossRef]
50. Nemati, M.; Lowenadler, J.; Harrison, S.T.L. Particle size effects in bioleaching of pyrite by acidophilic thermophile *Sulfolobus metallicus* (BC). *Appl. Microbiol. Biotechnol.* **2000**, *53*, 173. [CrossRef]
51. Rawlings, D.; Tributsch, H.; Hansford, G. Reasons why "*Leptospirillum*"-like species rather than *Thiobacillus ferrooxidans* are the dominant iron-oxidizing bacteria in many commercial processes for the biooxidation of pyrite and related ores. *Microbiol.* **1999**, *145*, 5. [CrossRef]
52. Mousavi, S.M.; Yaghmaei, S.; Salimi, F.; Jafari, A. Influence of process variables on biooxidation of ferrous sulfate by an indigenous *Acidithiobacillus ferrooxidans*. Part I: Flask experiments. *Fuel* **2006**, *85*, 2555–2560. [CrossRef]
53. Dopson, M. Growth in sulfidic mineral environments: Metal resistance mechanisms in acidophilic micro-organisms. *Microbiology* **2003**, *149*, 1959. [CrossRef] [PubMed]
54. Pogliani, C.; Donati, E. The role of exopolymers in bioleaching of a non-ferrous metal sulphide. *J. Ind. Microbiol. Biotechnol.* **1999**, *22*, 88. [CrossRef]
55. Dutrizac, J.E. Factors affecting alkali jarosite precipitation. *Metall. Trans. B* **1983**, *14*, 531–539. [CrossRef]
56. Dutrizac, J.E.; Dinardo, O. The co-precipitation of copper and zinc with lead jarosite. *Hydrometallurgy* **1983**, *11*, 61–78. [CrossRef]
57. Rohwerder, T.; Gehrke, T.; Kinzler, K.; Sand, W. Bioleaching review part A: Progress in bioleaching: Fundamentals and mechanisms of bacterial metal sulfide oxidation. *App. Microbiol. Biotechnol.* **2003**, *63*, 239. [CrossRef]